15th AIAA Computational Fluid Dynamics Conference
11-14 June 2001 Anaheim, CA

A01-31119

AIAA 2001-2655

Two-Dimensional Implicit Time Dependent Calculations for Incompressible Flows on Adaptive Unstructured Meshes

P. Lin * L. Martinelli † T.J. Baker ‡
Princeton University, Princeton, NJ 08544 U.S.A.

A. Jameson §
Stanford University, Stanford, CA 94305 U.S.A.

An implicit multigrid-driven algorithm for two-dimensional incompressible laminar viscous flows is coupled with a mesh adaptation method to better capture the important features of the flow for time dependent problems. Time dependent calculations are performed implicitly by regarding each time step as a steady-state problem in pseudotime. The method of artificial compressibility is used to solve the flow equations. An adaptation method performs local mesh refinement using an incremental Delaunay algorithm and mesh coarsening by means of an edge collapse. The method is validated by comparison with experimental results of low Reynolds number flow over a shedding circular cylinder.

Introduction

Over the past 10-15 years there has been a large amount of interest in numerically simulating time dependent phenomena. Time dependent phenomena are important in a variety of compressible and incompressible flows. Examples include flutter analysis, free surface flows, turbulent flows, unsteady wake flows, and time dependent geometries such as helicopter rotor blades, propellers, or compressor and turbine blades.

For the calculation of time dependent flows, implicit methods offer the the advantage of having the size of the time step be dictated by the physics of the flow rather than stability considerations, in contrast with explicit methods. Jameson[19] proposed a fast and efficient way to calculate time dependent flows using a multigrid-driven dual time stepping scheme. This method was improved by Melson et. al.[30] and has been used successfully in the study of aeroelastic problems,[1] in the study of low Reynolds number wake flows,[7] for the calculation of free surface flows with plunging breakers,[24] and for the calculation of high speed compressible flows.[23] This method has also been used for unstructured meshes.[22–24,37,38]

In a true incompressible flow the acoustic speed is infinite. The disparity in the acoustic and convective wave speeds make the system of equations ill-conditioned. A preconditioning matrix can be introduced to reduce this disparity in the wave speeds. Chorin[10] proposed the method of artificial compressibility for steady state problems, which was later modified to treat time dependent problems.[31,33,36] This artificial compressibility approach has also been used successfully with Jameson's implicit multigrid-driven dual time time stepping method.[7,22,24]

In most flow solutions there tends to be a large disparity in length scales which will require the mesh to also have a large disparity in mesh size. One of the problems of generating a grid that requires a large disparity in mesh size is that one needs some a priori knowledge of the solution to be able to place grid points where there will be high gradients. However, one usually does not know a priori where the regions of fine resolution are necessary, and for the case of a time dependent problem, there is the additional problem that regions where fine resolution is necessary can change position.[25] An example is unsteady laminar flow over a cylinder at low Reynolds number. Vorticies are shed from the cylinder in a periodic manner. Ideally we would want the grid to be fine only where the vorticies are located and coarse elsewhere.

For a general purpose method, we are left with ei-

*Graduate Student, Department of Mechanical and Aerospace Engineering, AIAA member

†Associate Professor, Department of Mechanical and Aerospace Engineering, AIAA Associate Fellow

‡Senior Research Scientist, Department of Mechanical and Aerospace Engineering

§Thomas V. Jones Professor of Engineering, Department of Aeronautics and Astronautics, AIAA Fellow

ther having a uniformly fine grid everywhere which is clearly a waste of computational resources if there are large regions of the flow with low gradients, or alternatively with using adaptive techniques. Spending all one's effort to make a flow solver faster and more efficient may not produce large benefits if mesh points are inefficiently placed or even worse, if certain important flow features are not resolved because the mesh is too coarse in that region. Therefore, efficient and accurate numerical computation requires both a fast and efficient flow solver and an adaptation scheme. Mesh adaptation for unsteady problems has stricter requirements than steady problems with regards to speed and efficiency of the algorithm as well as storage requirements as compared with steady problems.[25]

Mesh adaptation can be broken into three types of modification: changing the order of accuracy of the discretized approximation (p-refinement), changing the number of points by insertion and deletion (h-refinement), and by rearranging the distribution of points (r-refinement). The last two modifications involve altering the mesh. Often more than one type of refinement will be used. Among the adaptation methods that alter the mesh, h-refinement is considered to be the preferred method of adaptation.[3] The two main approaches for h-refinement for unstructured meshes of triangles in two dimensions or tetrahedra in three dimensions is by insertion of new points on the edges[6,8,11–13,21,25] and by insertion of new points by a Delaunay based method.[16,23,26,28,32] The former approach offers the advantage of being straightforward to implement. The latter approach is more flexible because it allows points to be inserted anywhere rather than being constrained to insertion on an edge.[3]

Unsteady incompressible wake flows for low Reynolds number flows are being actively studied both through experiment[15,39–42] and numerical simulation.[7,18] Belov et. al.[7] studied wake flows using a structured flow solver and obtained excellent results. However, one problem that they found was that sometimes the flow features in the far wake were underresolved due to the large cell sizes in the far wake. The natural next step is to use an adaptive mesh method. Henderson[18] used an unstructured spectral element method to study wake flows. He also extended his method to include an adaptive approach.[17]

The present work extends the first author's earlier work concerning time dependent incompressible flows with an unstructured grid[22] to study wake flows. The numerical method used couples the fast and efficient multigrid-driven implicit method of Jameson[19] and the method of artificial compressibility of Chorin[10] with an extension of the h-refinement mesh adaptation approach of Baker.[4] This mesh adaptation approach uses a Delaunay based coarsening and refinement technique for flexibility and to maintain good grid quality. The second reason this mesh adaptation procedure was chosen is because this approach determines whether deletion or enrichment should occur based on the fraction of standard deviation that the error indicator is above or below the mean and is a first step towards a more automated way of deciding which points should be deleted or inserted rather than an approach that requires the user to supply the upper and lower thresholds for an error indicator or detector. The Voronoi segment method of Rebay[34] is used for enrichment. One advantage of using a dual time stepping approach with mesh adaptation is that because mesh adaptation occurs during each pseudo-transient calculation to determine the solution for the next physical time step, there is no time lag between the adapted mesh and the flow solution in physical time. To validate this method and to demonstrate how this method can be used to study wake flows, numerical computations are performed for unsteady incompressible flow around a cylinder for the Reynolds number range of $50 \leq Re \leq 175$ and compared with experimental results.[39,41,42]

Numerical Discretization

The governing equations of concern are the time-dependent incompressible Navier-Stokes equations in two dimensions. We will be considering laminar, constant viscosity flow without body forces. For a homogeneous incompressible flow, density is constant and will be nondimensionalized to unity.

The governing equations in integral form for an arbitrary mesh with arbitrary mesh velocity are

$$\frac{d}{dt}\iint_{\Omega} \mathbf{t}\, d\Omega + \oint_{\partial\Omega} (\mathbf{f_i} - \mathbf{s_i})\, \partial\Omega = 0 \qquad (1)$$

where $\mathbf{t}$ is the vector

$$\mathbf{t} = \begin{pmatrix} 1 \\ u_1 \\ u_2 \end{pmatrix}$$

and the $\mathbf{f_i}$ and $\mathbf{s_i}$ are the Euler and the viscous flux vectors

$$\mathbf{f_i} = \begin{pmatrix} (u_i - u_{mesh_i}) \\ u_1(u_i - u_{mesh_i}) + p\delta_{1i} \\ u_2(u_i - u_{mesh_i}) + p\delta_{2i} \end{pmatrix}, \quad \mathbf{s_i} = \begin{pmatrix} 0 \\ \tau_{i1} \\ \tau_{i2} \end{pmatrix}.$$

Ω represents the control volume and $\partial\Omega$ represents the boundary of the control volume.

The dimensionless viscous stress tensor is

$$\tau_{ij} = \frac{1}{Re}\left(\frac{\partial u_i}{\partial x_j} + \frac{\partial u_j}{\partial x_i}\right)$$

where $Re = \frac{U_\infty L}{\nu}$ is the Reynolds number, ν is the kinematic viscosity, and U_∞ and L are the characteristic velocity and the length scales of the problem.

The governing equations are discretized by a finite volume scheme on unstructured triangular meshes. The flow variables are stored at the nodes and the control volumes are the nonoverlapping polygons that surround the nodes. The contour integral of the convective and viscous terms are computed using the trapezoidal rule. This technique can be shown to be equivalent to a Galerkin finite-element discretization with linear elements under certain conditions.[5,29,38] Discretization of the convective and viscous terms produces the following form

$$\frac{d}{dt}\iint_\Omega \mathbf{t}\, d\Omega + \mathbf{R}(\mathbf{w}) = 0$$

where the residual $\mathbf{R}(\mathbf{w})$ is the sum of the convective and viscous fluxes. Note that the residual is the function of the flow vector $\mathbf{w}$ rather than the vector $\mathbf{t}$, where

$$\mathbf{w} = \begin{pmatrix} p \\ u_1 \\ u_2 \end{pmatrix}.$$

Details of the discretization are provided in the references.[5,29]

To prevent odd-even decoupling in regions of the flow where the convective term dominates, it is necessary to add artificial dissipation. Artificial dissipation is calculated along the edges.[20] Because there are no discontinuities in the flow, first order dissipation will not be used. An undivided biharmonic operator of the flow variables is used to provide third order dissipation. The dissipation at point i is computed by the following sum over all the nodes that it shares an edge with

$$\mathbf{D}_i(\mathbf{w}) = \sum_j \mu_4 \rho_{ij}(\nabla^2\mathbf{w}_j - \nabla^2\mathbf{w}_i)$$

where ∇^2 is the undivided Laplacian

$$\nabla^2\mathbf{w}_i = \sum_j (\mathbf{w}_j - \mathbf{w}_i).$$

μ_4 is a dissipation coefficient and ρ_{ij} is a scale factor that will be discussed below. An alternative artificial dissipation scheme was also implemented that is based on a characteristic decomposition approach or a "matrix dissipation" approach.

Assuming that the flow variables are constant over each control volume for the time derivative term gives the semi-discrete equation

$$\frac{d}{dt}[\mathbf{t}V] + \mathbf{R}(\mathbf{w}) = 0.$$

For each control volume, we will solve this equation at each mesh point in an implicit manner

$$\frac{d}{dt}[\mathbf{t}^{n+1}V^{n+1}] + \mathbf{R}(\mathbf{w}^{n+1}) = 0.$$

In this work, $\frac{d}{dt}$ is discretized as a k-th order accurate backward difference formula defined by

$$\frac{d}{dt} = \frac{1}{\Delta t}\sum_{q=1}^{k}\frac{1}{q}(\Delta^-)^q$$

where

$$\Delta^-\mathbf{w} = \mathbf{w}^{n+1} - \mathbf{w}^n.$$

Both the second and third order accurate difference operators were used. The second order discretization in time gives

$$\frac{1}{\Delta t}(a_1[\mathbf{t}^{n+1}V^{n+1}] + a_2[\mathbf{t}^nV^n] + a_3[\mathbf{t}^{n-1}V^{n-1}] + a_4[\mathbf{t}^{n-2}V^{n-2}]) + \mathbf{R}(\mathbf{w}^{n+1}) = 0.$$

where $\mathbf{a} = (3/2, -2, 1, 0)$ and is A-stable.
$\mathbf{a} = (11/6, -3, 3/2, -1/3)$ give the third order discretization in time which is stiffly stable. It is convenient to define the modified residual as follows

$$\mathbf{R}^*(\mathbf{w}) = \frac{1}{\Delta t}\sum_{q=1}^{4} a_q\mathbf{t}^{n-q+2} + \mathbf{R}(\mathbf{w}).$$

The method of artificial compressibility is used to both convert the hyperbolic-elliptic unsteady incompressibility Navier-Stokes equations to a hyperbolic-parabolic system and to reduced the disparity in the wave speeds of the system. The advantage of converting the hyperbolic-elliptic system to a hyperbolic-parabolic system is that efficient techniques for solution of hyperbolic-parabolic systems can be used. The modified residual is multiplied by a local preconditioning matrix and a pseudo-unsteady term is added to give

$$\frac{d}{dt^*}[\mathbf{w}V] + \mathbf{Pr}\cdot\mathbf{R}^*(\mathbf{w}) = 0$$

where

$$\mathbf{Pr} = \begin{pmatrix} \beta^2 & 0 & 0 \\ 0 & 1 & 0 \\ 0 & 0 & 1 \end{pmatrix}.$$

The purpose of adding the pseudo-unsteady term is so we can treat the advancement to the next physical time step as solving a steady-state problem in pseudotime t^*. β is the artificial compressibility parameter and is chosen to improve the rate of convergence.

Following the work of Rizzi and Eriksson[35] and later Dreyer,[14] we scale β by the local velocity as follows

$$\beta^2 = max(0.25, u_1^2 + u_2^2)$$

From[36] the eigenvalues of our system are

$$\lambda_1 = U_n - u_{mesh}$$

$$\lambda_2 = U_n - \frac{1}{2}u_{mesh} + a_n$$

$$\lambda_3 = U_n - \frac{1}{2}u_{mesh} - a_n$$

where

$$U_n = \mathbf{u} \cdot \mathbf{n}$$

$$u_{mesh} = \mathbf{u}_{mesh} \cdot \mathbf{n}$$

$$a_n = \sqrt{(U_n - \frac{1}{2}u_{mesh})^2 + \beta^2(\Delta x^2 + \Delta y^2)}$$

and $\mathbf{n}$ is the normal to the edge and Δx and Δy are the differences between the two endpoints for each edge. The scale factor for each edge ρ_{ij} is the largest eigenvalue and is used for scaling the artificial dissipation as well as calculating the time step.

A five stage point-implicit Runge-Kutta type scheme[30] is used to solve these equations to steady-state in pseudotime.

During the evolution to steady-state in pseudotime, the solution is not time dependent, so various convergence acceleration can be used. The three used in this work are multigrid, local time stepping, and residual averaging. Details are provided in the references.[22,27]

The no-slip boundary condition is enforced at solid boundaries. A vertex-based version of the approximate non-reflecting far-field boundary conditions used by Belov et. al.[7] is used for the outer boundary of the domain. These are based on a linearized characteristics approach.

Mesh Generation and Adaptation

Initial Mesh Generation

The initial mesh generation is based on a constrained Delaunay triangulation.[2,26] The goal is to obtain a smooth gradation in mesh generation throughout the domain such that the density of the volume mesh near the boundary surface matches the mesh size of the boundary triangulation.[4] The length density function ρ at each point is related to the target circumradius of triangles in that region. The initial mesh generation proceeds as follows. Points are placed on the boundaries in a certain manner and then an initial triangulation of the volume is generated without any interior points. The initial length density function for the boundary points is calculated as an average length of the incident boundary edges. As interior points are added, the length density function of the new point is assigned the weighted average of the verticies of the triangle that contains the new point. Points are inserted if the actual circumradius is a certain threshold larger than the length density function. Interior points are added by the Voronoi segment method of Rebay.[34] Figure 1 and Figure 2 give an example of an initial mesh generated around a circular cylinder. The former shows the entire mesh while the latter is a close-up of the mesh around the cylinder. The cylinder has 128 points on its surface while the far field outer boundary has 64 points and is 16.7 cylinder diameters from the center of the cylinder. There are 2300 mesh points in this example initial grid.

Mesh Adaptation

Central to any mesh adaptation scheme are two essential requirements, a means of recognizing where extra flowfield resolution is needed and, secondly, a mechanism to alter the mesh in an appropriate manner.[3]

As the goal of an adaptation scheme is to achieve error equidistribution at all the mesh points, the first requirement will be fulfilled by using an error indicator that is based on a finite volume discretization of the second derivative of an appropriate flow quantity.[23,25] Because wake flows will be studied in this work, the flow quantity chosen is total pressure. Before adaptation occurs, the value of the error indicator E is calculated at each node.

Because the size of triangles is controlled by the length density function ρ, which represents a target circumradius, we need a mechanism to modify ρ. Using a modified version of the method of Baker,[4] the average error indicator for the entire mesh $\bar{E}$ is computed and the the standard deviation σ is calculated from $\sigma^2 = \bar{E^2} - \bar{E}^2$. Let

$$e_{up} = \frac{E - \bar{E} - \lambda_{up}\sigma}{\sigma}$$

$$e_{low} = \frac{E - \bar{E} + \lambda_{low}\sigma}{\sigma}$$

Then the new ρ at each mesh point becomes

$$\rho_{new} = \begin{cases} \frac{\rho}{1+\alpha min(e_{up},1)} & E > \bar{E} + \lambda_{up}\sigma \\ \rho & \bar{E} - \lambda_{low}\sigma \leq E \leq \bar{E} + \lambda_{up}\sigma \\ \rho * B & E < \bar{E} - \lambda_{low}\sigma \end{cases}$$

$$B = [1 + \alpha min(abs(e_{low}), 1)]$$

λ_{up} is the fraction of a standard deviation above the mean where the length density function starts to be decreased (increasing the likelihood and amount of enrichment), λ_{low} is the fraction of a standard deviation below the mean where the length density function starts to be increased (increasing the likelihood and amount of coarsening), and α controls how rapidly changes in mesh density occur. A larger value of α will cause a larger change in mesh density. λ_{up}, λ_{low}, and α are user supplied constants. If the ratio of a triangle's circumradius to ρ_{new} is above a certain threshold, then the triangle is classified as a nonaccepted triangle. The edge between a nonaccepted and accepted triangle is flagged for point insertion by the Voronoi segment method of Rebay.[34] If this ratio falls below a certain threshold, then the triangle will be deleted.

The second requirement of an adaptation scheme is a mechanism to alter the mesh. This is also based on a modified version of the method of Baker.[4] Triangles that are to be deleted are deleted by collapsing its shortest edge which will actually delete two triangles. After all the necessary triangles are deleted, diagonals are swapped in order to maximize the minimum of the angles of the pair to triangles with a common edge that form a convex quadrilateral. Enrichment is accomplished by inserting a point using the Voronoi segment method and performing an incremental Delaunay algorithm.

The example mesh in the section on initial mesh generation (Figure 1 and Figure 2) is used as the starting point for a calculation of the incompressible flow over a circular cylinder at a Reynolds number of 150. Figure 3 shows the vorticity field for the entire domain with the mesh allowed to adapt and and Figure 4 shows the adapted grid for the entire domain once periodic shedding has been obtained. Figure 5 shows the vorticity field for the portion of the domain near the cylinder and and Figure 6 shows the corresponding adapted grid. For the sake of comparison, Figure 7 shows the vorticity field once periodic shedding has been obtained but with no mesh adaptation (compare this with Figure 3). The adapted mesh for this example typically had around 7000–7200 points. Recall that the initial mesh had 2300 points so the number of mesh points was increased by roughly a factor of three. Note that the refined portions of the grid seem to track the important features of the flow field.

Multigrid and Mesh Adaptation

Multigrid requires the generation of a sequence of coarser meshes. The generation of a sequence of coarser meshes is more difficult with a dynamically adapting mesh. The approach for handling the coarser meshes for multigrid is as follows. Mesh adaptation is performed on the the finest grid only. The coarser grids for multigrid are then derived from the finest grid using a coarsener. As a first attempt for a coarsener, a fast simple coarsener that is based on initial triangulation techniques rather than edge collapsing techniques is used.

The method is based on generating coarser meshes for a vertex-based structured code in two dimensions. For the structured case, the coarser grid is generated by removing every other point in each direction, doubling the spacing between each point in both directions. This reduces the amount of points to $\frac{1}{4}$ the original number.

In analogy to the structured case, we want to roughly double the spacing between each point on a fine mesh to generate a coarser mesh. The average edge length of all edges incident to each point is calculated. This gives a rough distance measure to the neighboring points. The coarser grid is generated first by removing every other boundary point on the fine grid and then an initial triangulation is produced. Using a Bowyer algorithm,[9] an attempt is made to insert each interior point of the fine grid. A comparison is made between the distance of the potential new point to the closest existing coarse grid point and the average associated edge length of that existing coarse grid point multiplied by a factor. If the former is greater than the latter, then the potential new point becomes a coarse grid point, otherwise it is rejected.

This coarsener relies on pure geometric considerations to produce a coarse mesh. An advantage is that it should produce a coarse mesh that closely resembles the fine mesh. Because the coarsener needs to be called each time after adaptation occurs on the finest mesh, the coarsener needs to be fast, otherwise this method will be inefficient. The key to the speed

of the coarsener is a quadtree data structure.[2]

Results

Validation of the basic flow solver without mesh adaptation and viscous effects was presented in one of the references.[22] Here, we will discuss validation of the viscous portion of the flow solver and the mesh adaptation portion.

One of the benchmark test cases for any unsteady incompressible laminar Navier-Stokes algorithm is flow over a circular cylinder due to the amount of experimental[39,41,42] and computational[7,18] data available. Experiments conducted by Williamson,[39] indicate that the flow around a circular cylinder does not become unsteady until a critical Reynolds number of about $Re_c = 49$. Spanwise independent parallel shedding is observed in the approximate range of $49 < Re < 180$, above which three-dimensional shedding modes are observed. This makes the range $49 < Re < 180$ useful for validating two-dimensional unsteady algorithms. Williamson[39] proposed a relation for Strouhal frequency, St(Re), of the form

$$St(Re) = \frac{A}{Re} + B + C \cdot Re$$

where A, B, and C are constants ($A = -3.3265$, $B = .1816$, $C = 1.600 \times 10^{-4}$). This relationship fits Williamson's experimental data to within about 2%.[41]

Computations were performed using an initial grid that contains twice the number of body points as shown in the example grid when describing the initial mesh generation. 256 points were equally spaced around the cylinder and 64 points were equally spaced around the far field outer boundary. The total number of mesh points for the initial grid was 3200. Once periodic shedding was reached, the total number of mesh points was 9900–10200 for the $Re = 50$ case and 14200–15200 for the $Re = 175$ case, with the other cases being somewhere in between. The third order backward time discretization was used, with 48 time steps per shedding cycle. The mesh coarsener was used to generate the coarser grids for multigrid.

Figure 8 shows the comparison between this experimental data and the computational results. Strouhal frequency is plotted on the vertical axis with Reynolds number, Re, on the horizontal axis. The solid line is the best fit of the experimental data to the relation $St(Re) = \frac{A}{Re} + B + C \cdot Re$. The computed Strouhal number is within 2% of the above best fit to the experimental data, and the computed St differs by 1% or less for the Re between 60 and 150. The computational results agree well with the experimental results.

Williamson and Roshko[42] also proposed a relationship of the same form but with different coefficients for average base pressure coefficient $Cpb(Re)$ with Reynolds number ($A = -14.3500, B = .6950, C = 16.920$). Note that these coefficients were obtained from the work of Henderson.[18] Figure 9 shows the comparison between the above best fit to the experimental data and the computational results. Base pressure coefficient is plotted on the vertical axis with Reynolds number, Re, on the horizontal axis. The solid line is the best fit of the experimental data to the relation $St(Re) = \frac{A}{Re} + B + C \cdot Re$. The computed base pressure is within 5% of the best fit curve to the experimental data and is consistently lower.

Conclusion

This work extended the first author's previous work involving time dependent calculations for incompressible Euler flows on unstructured meshes to include laminar viscous effects and to improve resolution of the flow field by adding a mesh adaptation method. Validation of the method with unsteady periodic shedding of a circular cylinder in the Reynolds number range of $49 < Re < 180$ show that the mesh adaptation method is able to track the vorticies as they convect downstream and out of the domain and that the Strouhal frequency and base pressure coefficient agree with experimental results. The success with the circular cylinder shows that this method may hold promise for studying other wake flows such as behind half cylinders or flapping airfoils.

Acknowledgements

The first author wishes to thank Dr. Biing-horng Liou for his generous help and Professor C.H.K. Williamson for providing his experimental data. The first author is grateful for the generous support of the Guggenheim Fellowship Program for one year and the Office of Naval Research for several years.

References

[1]J.J. Alonso, L. Martinelli, and A. Jameson. Multigrid unsteady Navier-Stokes calculations with aeroelastic applications. *AIAA Paper 95-0048*, 33rd Aerospace Sciences Meeting, Reno, NV, January 1995.

[2]T.J. Baker. Automatic mesh generation for complex three-dimensional regions using a constrained Delaunay triangulation. *Engineering with Computers*, 5:pp. 161–175, 1989.

[3]T.J. Baker. Mesh adaptation strategies for problems in fluid dynamics. *Finite Elements in Analysis and Design*, 25:pp. 243–273, 1997.

[4]T.J. Baker. Mesh modification for solution adaptation and time evolving domains. Whistler, British Columbia,

Canada, 2000. 7th International Conference on Numerical Grid Generation in Computational Field Simulations.

[5]T.J. Barth. Aspects of unstructured grids and finite-volume solvers for the Euler and Navier-Stokes equations. *AGARD Report 787 Special Course on Unstructured Grid Methods for Advection Dominated Flows*, pages 6–1—6–61, 1992.

[6]J.D. Baum and L. Lohner. Numerical simulation of shock interactions with a modern main battlefield tank. *AIAA Paper 91-1666*, 22nd AIAA Fluid Dynamics, Plasma Dynamics and Lasers Conference, Honolulu HI, 1991.

[7]A. Belov, A. Jameson, and L. Martinelli. Three-dimensional unsteady incompressible flow calculations using multigrid. *AIAA Paper 97-0443*, 35th Aerospace Sciences Meeting, Reno, NV, January 1997.

[8]R. Biswas and R. Strawn. A new procedure for dynamic adaption of three-dimensional unstructured grids. *Applied Numerical Mathematics*, 13:pp. 473–452, 1994.

[9]A. Bowyer. Computing Dirichlet tessellations. *The Computer Journal*, 24(2):pp. 162–166, 1981.

[10]A.J. Chorin. A numerical method for solving incompressible viscous flow problems. *Journal of Computational Physics*, 2:pp. 12–26, 1967.

[11]S.D. Connell and D.G. Holmes. A 3D unstructured adaptive multigrid scheme for the Euler equation. *AIAA Paper 93-3339-CP*, 11th AIAA Computational Fluid Dynamics Conference, Orlando FL, 1993.

[12]H.L. De Cougny and M.S. Shephard. Parallel refinement and coarsening of tetrahedral meshes. *International Journal for Numerical Methods in Engineering*, 46:pp. 1101–1125, 1999.

[13]M. Delanaye and J.A. Essers. An accurate finite volume scheme for Euler and Navier-Stokes equations on unstructured adaptive grids. *AIAA Paper 95-1710-CP*, 12th AIAA Computational Fluid Dynamics Conference, San Diego CA, 1995.

[14]J.J. Dreyer. Finite volume solutions to the steady incompressible Euler equations on unstructured triangular meshes. Master's thesis, Princeton University, Princeton, NJ, June 1990.

[15]M. Hammache and M. Gharib. An experimental study of the parallel and oblique vortex shedding from circular cylinders. *Journal of Fluid Mechanics*, 232:pp. 567–590, 1991.

[16]O. Hassan, L. Bayne, K. Morgan, and N. Weatherill. An adaptive unstructured mesh method for transient flows involving moving boundaries. Technical report, Eccomas 98, September 1998.

[17]R. Henderson and D. Meiron. Dynamic refinement algorithms for spectral element methods. *AIAA Paper 97-1855*, 13th AIAA Computational Fluid Dynamics Conference, Snowmass CO, 1997.

[18]R.D. Henderson. *Unstructured Spectral Element Methods: Parallel Algorithms and Simulations.* PhD thesis, Princeton University, Department of Mechanical and Aerospace Engineering, June 1994.

[19]A. Jameson. Time dependent calculations using multigrid, with applications to unsteady flows past airfoils and wings. *AIAA Paper 91-1596*, 10th AIAA Computational Fluid Dynamics Conference, Honolulu, HI, June 1991.

[20]A. Jameson, T.J. Baker, and N.P. Weatherill. Calculation of inviscid transonic flow over a complete aircraft. *AIAA Paper 86-0103*, 24th AIAA Aerospace Sciences Meeting, Reno NV, January 1986.

[21]Y. Kallinderis and P. Vijayan. Adaptive refinement-coarsening scheme for three-dimensional unstructured meshes. *AIAA Journal*, 31(8), 1993.

[22]P. T. Lin. Implicit time dependent calculations for compressible and incompressible flows on unstructured meshes. Master's thesis, Princeton University, Princeton, NJ, November 1994.

[23]B.-H. Liou and D. Balsara. An implicit unstructured adaptive-grid approach for compressible flows with moving boundaries. *AIAA Paper 2001-0440*, 39th AIAA Aerospace Sciences Meeting and Exhibit, Reno, NV, January 2001.

[24]B.-H. Liou, L. Martinelli, T.J. Baker, and A. Jameson. Calculation of plunging breakers with a fully-implicit adaptive-grid method. *AIAA Paper 98-2968*, 29th AIAA Fluid Dynamics Conference, Albuquerque, NM, 1998.

[25]R. Lohner. An adaptive finite element scheme for transient problems in CFD. *Computer Methods in Applied Mechanics and Engineering*, 61:pp. 323–338, 1987.

[26]D.L. Marcum and N.P. Weatherill. Unstructured grid generation using iterative point insertion and local reconnection. *AIAA Journal*, 33(9):pp. 1619–1625, September 1995.

[27]D.J. Mavriplis. Multigrid solution of the 2-D Euler equations on unstructured triangular meshes. *AIAA Journal*, 26(7):pp. 824–831, July 1988.

[28]D.J. Mavriplis. Turbulent flow calculations using unstructured and adaptive meshes. *International Journal for Numerical Methods in Fluids*, 13:pp. 1131–1152, 1991.

[29]D.J. Mavriplis, A. Jameson, and L. Martinelli. Multigrid solution of the Navier-Stokes equations on triangular meshes. *AIAA Paper 89-0120*, 27th AIAA Aerospace Sciences Meeting, Reno NV, 1989.

[30]N.D. Melson, M.D. Sanetrik, and H.L. Atkins. Time-accurate Navier-Stokes calculations with multigrid acceleration. In *Proceedings of the 6th Copper Mountain Conference on Multigrid Methods*, Copper Mountain, CO, 1993.

[31]C.L. Merkle and M. Athavale. Time-accurate unsteady incompressible flow algorithms based on artificial compressibility. *AIAA Paper 87-1137*, 8th AIAA Computational Fluid Dynamics Conference, Honolulu, HI, June 1987.

[32]T.J. Mitty, A. Jameson, and T.J. Baker. Solution of three-dimensional supersonic flowfields via adapting unstructured meshes. *Computers Fluids*, 22(2/3):pp. 271–283, 1993.

[33]R.J. Peyret. Unsteady evolution of a horizontal jet in a stratified fluid. *Journal of Fluid Mechanics*, 78:49–63, 1976.

[34]S. Rebay. Efficient unstructured mesh generation by means of Delaunay triangulation and Bowyer-Watson algorithm. *Journal of Computational Physics*, 106:pp. 125–138, 1993.

[35]A. Rizzi and Lars-Erik Eriksson. Computation of inviscid incompressible flow with rotation. *J. Fluid Mech.*, 153:pp. 275–312, 1985.

[36]S.E. Rogers and D. Kwak. Upwind differencing scheme for the time-accurate incompressible Navier-Stokes equations. *AIAA Journal*, 28(2):pp. 253–262, February 1990.

[37]J.C. Vassberg. A fast, implicit unstructured-mesh Euler method. *AIAA Paper 92-2693*, 10th AIAA Applied Aerodynamics Conference, Palo Alto, CA, June 1992.

[38]V. Venkatakrishnan and D. Mavriplis. Implicit method for the computation of unsteady flows on unstructured grids. *Journal of Computational Physics*, 127:pp. 380–397, 1996.

[39]C.H.K. Williamson. Defining a universal and continuous Strouhal-Reynolds number relationship of the laminar vortex shedding of a circular cylinder. *Physics of Fluids*, 31:pp. 2742–2744, 1988.

[40]C.H.K. Williamson. Oblique and parallel modes of vortex shedding in the wake of a circular cylinder at low Reynolds numbers. *Journal of Fluid Mechanics*, 206:pp. 579–627, 1989.

[41]C.H.K. Williamson and G. Brown. A series in $1/\sqrt{Re}$ to represent the Strouhal-Reynolds number relationship of the

cylinder wake. *Journal of Fluids and Structures*, 12:pp. 1073–1085, 1998.

[42]C.H.K. Williamson and A. Roshko. Measurements of base pressure in the wake of a cylinder at low Reynolds numbers. *Zeitschrift fur Flugwissenschaften und Weltraumforschung*, 14:pp. 38–46, 1990.

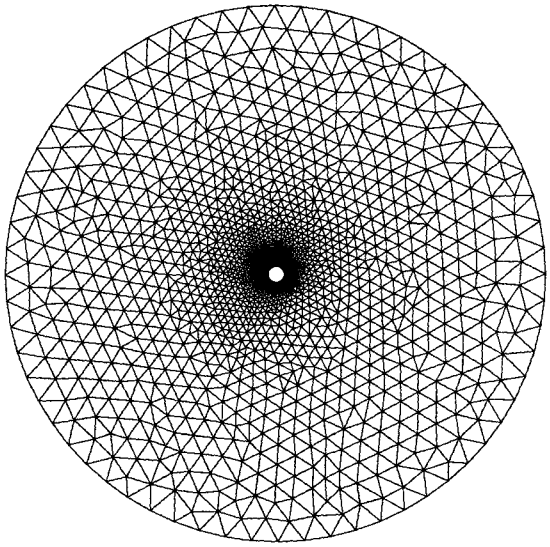

Fig. 1 Initial grid for circular cylinder

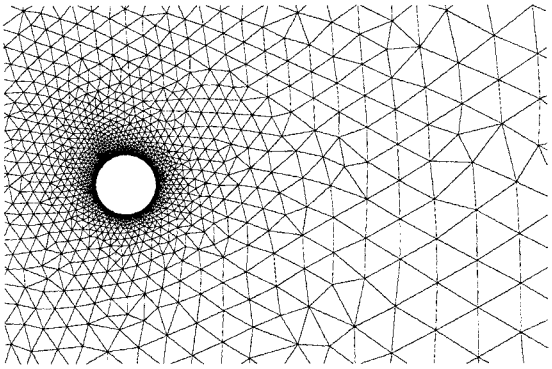

Fig. 2 Initial grid close up

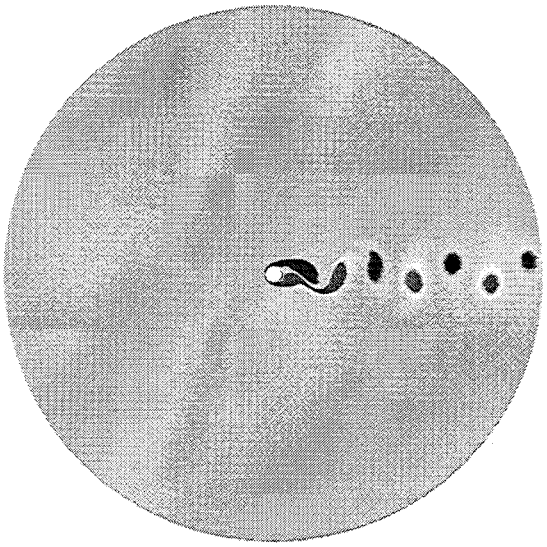

Fig. 3 Vorticity field with adaptation

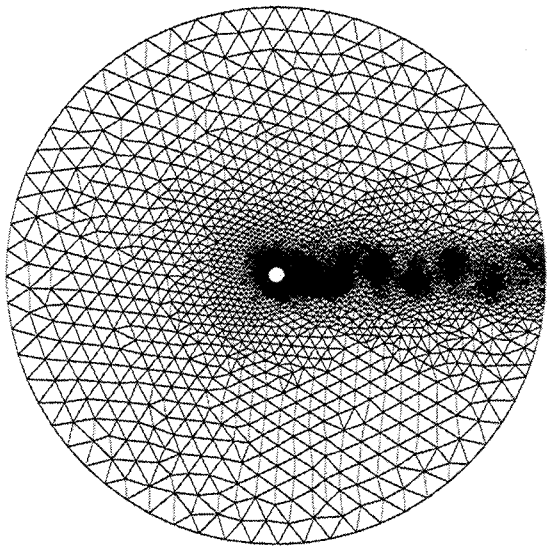

Fig. 4 Grid with adaptation

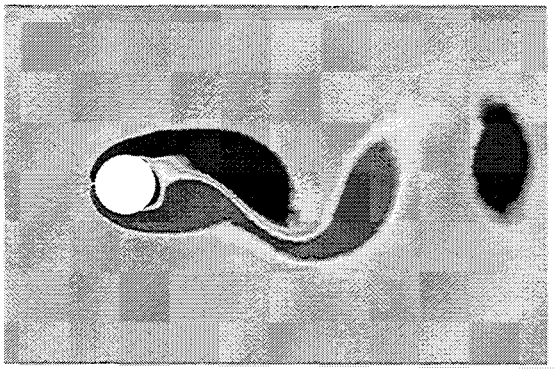

Fig. 5 Close up view of Vorticity field with adaptation

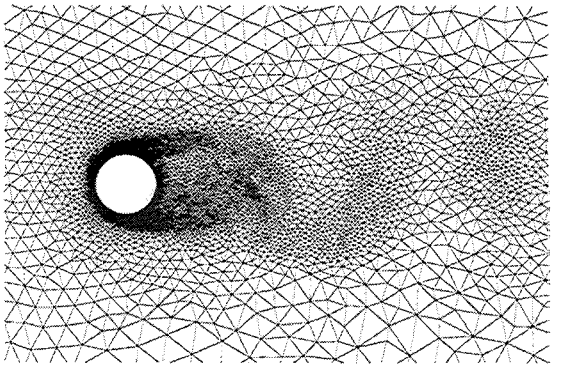

Fig. 6 Close up view of grid with adaptation

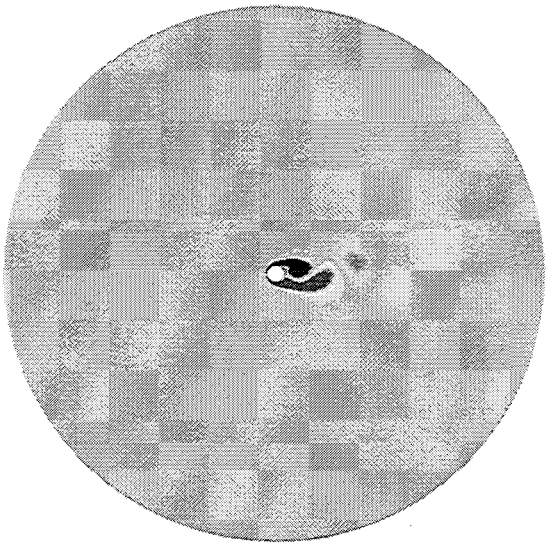

Fig. 7 Vorticity field with no adaptation

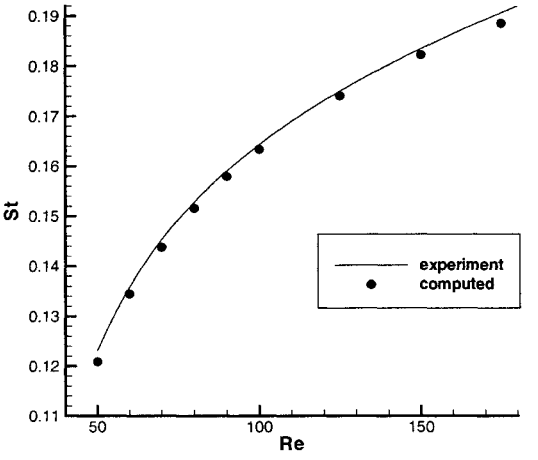

Fig. 8 St(Re) for circular cylinder $49 < Re < 180$

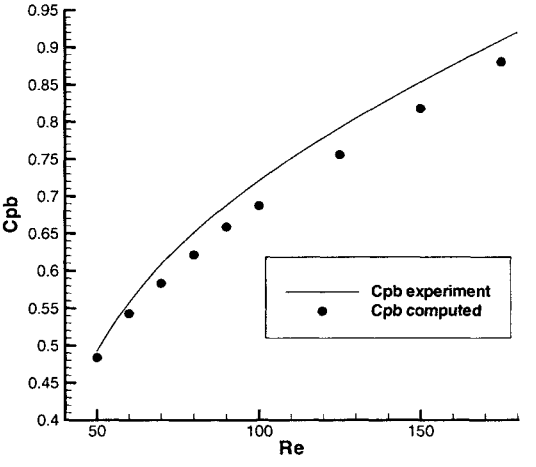

Fig. 9 Cpb(Re) for circular cylinder $49 < Re < 180$